

Local Stress Anomaly, their Interplay to Deep Seated Fault Structures and Geomechanical Characterization of Geothermal Reservoirs in southern Germany

Robin Seithel, Roman Schmidt, Thomas Kohl, Andreas Henk, Ingrid Stober

Adenauerring 20b, Building 50.40, 76131 Karlsruhe, Germany

[*Robin.Seithel@kit.edu](mailto:Robin.Seithel@kit.edu)

Keywords: Local stress anomaly, Upper Rhine Graben, fault zones, 1-D hydro mechanical Model, geomechanical modelling

ABSTRACT

Due to an increased heat flow and the presence of several aquifers, the Upper Rhine Graben (URG) offers favorable conditions for geothermal utilization and several geothermal projects have emerged in the last decade. Previous research in this tectonic setting proved that the hydraulic and geomechanical behavior of the geothermal reservoirs is mainly governed by the existence of meso-scale fractures and deep large-scale fault systems. The occurrence of induced seismicity as a result of fluid injection, however, clearly demonstrates that a better understanding on their role is still required.

The local stress field can be significantly influenced by the existence of fault zones. A good example of this behavior can be observed from a case study in the Molasse Basin. There, measured image logs in three geothermal wells demonstrate that the stress field in the vicinity of these reservoir structures can be perturbed. Fracture data as well as stress indicators were interpreted using these logs and analyzed to determine the local stress field. Two of the wells exhibited E-W and N-S fracture sets that correspond to the regional N-S oriented strike slip stress field of the Molasse Basin. The third well exhibited a markedly different fracture set that indicated a N-S oriented normal faulting regime. This secondary stress field is rotated 40° counter clockwise from the strike slip stress regime. The secondary fracture system and the stress regime are interpreted as a result of local stress changes influenced by existing fault structures.

This research aims to develop a better approach for characterization and parameterization of deep reaching faults and is intended to establish an improved understanding of their impact on reservoir mechanics. We perform geomechanical experiments (triaxial tests) with different rock types (granite and sedimentary rocks) to gain insight into fault parameterization and behavior under varying P/T conditions. Furthermore, geological field work on existing faults accessible in underground mines will be carried out to characterize these structures in-situ. Besides this lab and field approach, another focus lies on the development of site-specific numerical models to predict the stress distribution and the permeability evolution of large-scale fault systems over geologic time scales.

1. INTRODUCTION

The provinces with the highest geothermal potential in Germany, the Upper Rhine Graben and the Molasse Basin, are located in the North German Basin. Hydrothermal targets in the Molasse basin are typically Limestones within the Malm reservoir with high porosity as well as highly deformed fault structures. In the Upper Rhine Graben (URG), the main important hydrothermal aquifers are the Buntsandstein and the Upper Muschelkalk (Stober 2013). In the EGS-power plant at Soultz-Sous-Forêts the granitic crystalline basement rocks in the URG are used. Fault structures are thought to act potentially as reservoirs in this province (Stober et al. 2011). In the last decades, geothermal exploration in the Upper Rhine Graben (URG), Germany, became increasingly appealing because of the favorable temperature conditions and potential reservoir structures. The hydraulic conductivity in deep sedimentary units is usually thought to be insufficient for geothermal utilization, so highly deformed structures are often targets for deep geothermal energy projects.

Fault structures in the crystalline basement rocks can generally be divided into several categories depending on their deformation grade. Therefore, over a wide range of length the outer part of a fault zone has less fractures and is called the damage zone. The inner part is called the fault core, which is usually highly deformed, and may consist of gouge, cataclastic and ultracataclastic material with unordered fracture sets and reduced grain sizes (Mazurek et al. 2003; Caine et al. 2010). Fault zones can contain a single core or can be built up of several cores which are linked over a wide zone (Faulkner et al. 2003). The construction of these zones depends on the depth of formation, temperature, the protolith, tectonic environment, magnitude of displacement and fluid flow (Faulkner et al. 2010). Deformation mechanisms, induced by stress relief, will significantly change the petrophysical parameters. Both rock strength and permeability can change dramatically. After the faulting process, fluid flow occurs in zones with increased permeability and fluids circulate due to the gradient of hydraulic potential. Fluid chemistry of the hot water will affect the “fresh” rock surfaces and vice versa. Mineral alteration processes start, which can enhance matrix porosity or change fluid composition and lead to mineral precipitation and porosity reduction (Mazurek 1998; Bucher and Stober 2010).

Fracture density in crystalline basement rocks increases significantly from the outer damage zone to the inner fault core, which can act as weak zones (Gudmundsson et al. 2010). So, the Young's modulus for the highly-fractured inner core zone is low, increases in the less fractured outer damage zone, and is highest in the normally fractured protolith. Typically the inner fault core shows the weakest zone due to a concentrated deformation and the lowest grain size. Often in this zone mineral alteration and precipitation dominate petrophysical parameters and new mineral phases like clay are generated. A classical work for quantifying the strength of the crust is conducted by Byerlee (1978) providing a range of friction coefficients with fault slip displacement accompanied by brittle deformation. If faults show significantly lower friction coefficients than postulated by Byerlee they are called “weak” faults and tend to be seismogenically active. During our study we investigate in the URG as well faults in the Buntsandstein and the Upper Muschelkalk.

These altered mechanical parameters affect the local stress field in the vicinity of these fault zones. Homberg (1997) detected in particular those areas with modified stress field in direction and magnitude. Geological field studies verify this observation and detected areas with tensional and compressional stress indicators near to strike-slip fault zones. A simple model of a strike slip fault can show the stress configuration after a faulting process and describe the stress components near the fault tip. The modelled stress field identified especially high shear stresses in the vicinity of the strike slip fault tips (Chinnery 1965) with a stress concentration at the sides of this feature (Su and Stephansson 1999).

One aim of this study is to establish a 1-D geomechanical model of the reservoir rocks in the URG to better understand the faulting style, the mechanical behavior, and the influence on the hydraulic permeability of different kind of faulted rocks. Therefore, limestone as well as sandstone rock samples of the Trias (Muschelkalk, Buntsandstein) and granite from the Crystalline Basement will be investigated. First investigations are conducted with highly homogeneous undeformed samples from quarries in the Black Forest. Mechanical parameters like cohesion, friction angle and the young's modulus were determined with a triaxial press. We started with the confining pressures of 10 MPa and increased up to 30 MPa at room temperature. Afterwards we intend to expand our study on real reservoir conditions with a confining pressure of 100 MPa and temperature of 160 °C. To check and to enhance the validity of our study we will additionally analyze rock core samples of the Soultz-Sous-Forêts geothermal project possessing deep-seated fault zones.

2. LOCAL STRESS PERTURBATION

2.1 Stress perturbation affected by fault systems

Fault zones can have a significant influence on the stress field due to modified mechanical and hydraulic parameters caused by deformation processes. Thus, stress distribution results in contractional areas where stresses are getting concentrated and tensional areas where local stress concentration lead to lower stresses.

Depending on the mechanical contrast of the heterogenic to the undisturbed parameters, the orientation of the fault structures and especially the maximum horizontal stress will define the stress distribution around fault zones. At the small scale (single fractures) and at the large scale (fault zones), the stress pattern shows a symmetrical configuration relative to the center of the discontinuity. At the stress facing tip of the discontinuity, on the opposite block, a clockwise rotation of the maximum stress parallel to the fault with increasing magnitude occurs, on the stress facing block an anticlockwise rotation perpendicular to the fault with decreasing magnitude occurs (Homberg et al. 1997). The magnitude of stress perturbation depends on the angle of fault orientation to the maximum horizontal stress, differential stress, and the strength of the fault gouge. Thus a larger the differential stress and a lower frictional strength displacement will increase the resulting enhanced stress perturbation.

Observations on oil field data confirm as well the above mentioned stress distribution around fault structures (Yale 2003). In particular, stress rotations could be detected where the horizontal differential stress is marked or fault zones can be seen as seismically active. Therefore, the stress field can be locally changed in reservoirs and will induce faulting mechanisms, hydraulic conductivity variations, and seismicity.

2.2 Example of an affected stress field in the Molasse Basin

The stress field in the Molasse Basin was analyzed by using image logs of three wells, each roughly 4000 m deep, in the Upper Jurassic (Malm) aquifer of the biggest geothermal site south of Munich. The wells were highly deviated in the reservoir sections and span a triangle to west-west north (Th1), north (Th2) and to the south (Th3) (Figure 1). Well Th1 is the production well and Th2 and Th3 are the injection wells. Stress field in the Molasse Basin appears to be N-S oriented with a compressive character (Reinecker et al. 2010) and tectonic elements strike WSW-ENE and NW-SE (Figure 1). The first named fault zones are anti- and synthetic normal faults striking parallel to the Alpine Orogen, the second fault zones constrained to the eastern part of the basin, belong to a post Jurassic transpressive uplift.

Image logs in the reservoir sections were interpreted for natural fractures, drilling induced tensile fractures (DITF), and breakouts (BO). DITFs and BO can be used to determine the stress distribution even in highly deviated wells. DITF indicate the orientation of tensile stresses and BO the orientation of compressive stresses (Brudy and Zoback 1993). In highly deviated wells the stress distribution depends on the well trajectory and the stress field. To model the direction of tensile as well as compressive stress for a well trajectory with an assumed stress field, stresses must be transformed from the geographic coordinate system to the borehole system and the maximum and minimum tangential stress direction has to be determined (Peska and Zoback 1995). Thus, the observed and the modeled stress orientations occurring in a decisive stress field can be compared.

Due to the compressive character, caused by the Alpine push, the stress field can be roughly estimated as an N-S oriented strike-slip stress regime. Modelling the stress distribution in the three wells (Th1, Th2 and Th3) with the well trajectory and the strike-slip stress regime, stress indicators can give insights into the local stress regime. Observed natural fractures can indicate the local tectonic environment and can give insights into different tectonic areas. In Th1 a single N-S striking fracture system is detected. In contrast, the two other wells, which were oriented to north (Th2) and south (Th3), showed a main fracture direction striking E-W and a secondary orientation with a strike of N-S to NNE-SSW. Stress indicator data in Th2 and Th3 confirm the strike-slip stress regime. But comparison of observations to the model of the stress indicators in Th1 indicate a different stress regime. As mentioned above, perturbed stress regime can be marked by different orientation or by a change in stress magnitude. The modeling approach shows that the minimal horizontal stress has no decisive influence on the stress distribution in the wells. So a change in magnitude and orientation can give insights on the stress field in well Th1. This shows that the optimal stress regime can be rotated counter-clockwise of 40° or the magnitude of the maximum horizontal stress is reduced, so that a normal faulting stress regime exists locally.

In Figure 1 a conceptual model of the fault zones and the stress field is presented. The fracture data in Well Th2 and Th3 are determined by the background E-W and NNE-SSW oriented fracture system which strike in the same way as the interpreted fault zones from the Geothermal Atlas of Bavaria (STMWIVT 2010). Stress modeling of the stress indicators point to the regional N-S

oriented strike-slip stress regime in Th2 and Th3. Because of the nearly perpendicular orientation of the stress regime and the strike of the fault zones even low fault strength will perturb the stress regime significantly. In contrast, the fracture system observed in Th1 indicates a N-S oriented fracture system which can be observed as a connection of the southern and the northern normal fault. In the top part of the image log a great amount of breakouts occur which can indicate a lower rock strength and the vicinity to fault structures in the Malm reservoir. Due to the low angle between the direction of the maximum horizontal stress and strike of the fault zone the influence to the local stress field will be more significant. The stress configuration illustrated in Figure (1) with the NNE-SSW striking fault zone and its contractional and tensional areas can be seen as responsible for the observed stress regime.

The stress regime observed during the WSM in the Molasse Basin show a decidedly homogeneous N-S oriented strike-slip stress regime. However, this study shows that on reservoir scale the stress regime can vary, which can influence the hydraulic and mechanical behavior in the reservoir. If such stress distributions can be modeled before reservoir development the reservoir targets can be adapted and from stress induced well stability problems it can be very beneficial to a project. The first step in building up such a model is to determine the parameters of the host rock, undisturbed rocks and on the faulted rocks. A one-dimensional model of faulted and unfaulted rocks will be established in the following section.

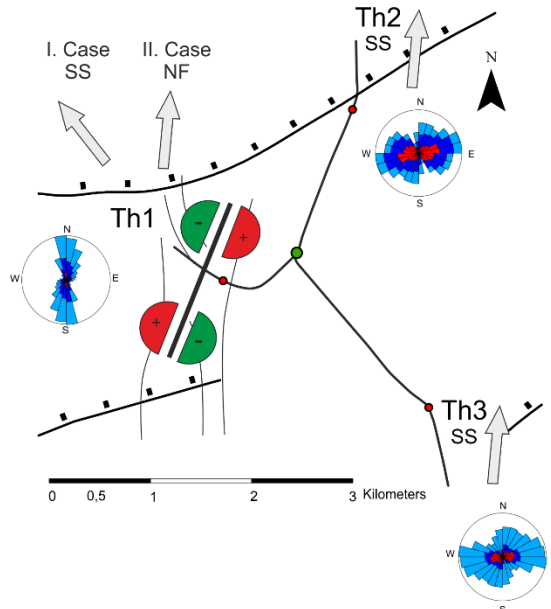


Figure 1: Conceptional model of the fracture system and the local stress system analyzed in a stress study of the wells. Additionally, the well paths and the top reservoir sections (red points) with the fault zones interpreted in the Bavarian Geothermal Atlas (STMWIVT 2010) are illustrated.

3. GEOMACHANICAL INVESTIGATIONS IN THE UPPER RHINE VALLEY

The above investigation was a case study on the possibility of altered local stress fields. The reservoirs in the URG consist of the granitic basement, the sandstones of the Buntsandstein layers and the limestones of the Muschelkalk, which can be described as fractured rock materials. For first mechanical characterization, rock samples from outcrops in the Black Forest, which represent the typical geothermal aquifers within the URG were analyzed.

3.1 Rock Samples

The outcrops were selected due to their stratigraphic classification and rock characteristic. Objectives for sample selection are homogeneity and small mineral size as well as isotropic petrophysical parameters. The map below shows the outcrops of the Muschelkalk (Figure 1, blue points), the Buntsandstein (Figure 1, yellow points) and the Basement (Figure 1, red points) which were selected for our investigation. Outcrop sampling was carried out according to the aforementioned criteria (Figure 1, black shadowed points). In our study, two different sandstones of the Buntsandstein, one from the northern Black Forest near to Wilferdingen called "Pfinztaeler Sandstein" (PfSst) and one from the central Black Forest called "Tennenbacher Sandstein" (TenSst) were selected. Limestones from the Muschelkalk are merely pervasive in the northern Black Forest. Many outcrops show thin layering, which cannot be used for our testing procedures. The relatively thick layering of the Keltener outcrop was much better suited to our investigations, so the focus is on the so called "Keltener Limestone" (KeKst). Crystalline Basement rocks are widespread throughout the entire Black Forest with granites as well as gneisses. The homogeneous and isotropic mineral distribution of the granites and especially the "Malsburg Granite" (MGrIa) were suited best to our investigations. Therefore, laboratory experiments were performed and will be carried out with this type of granite.

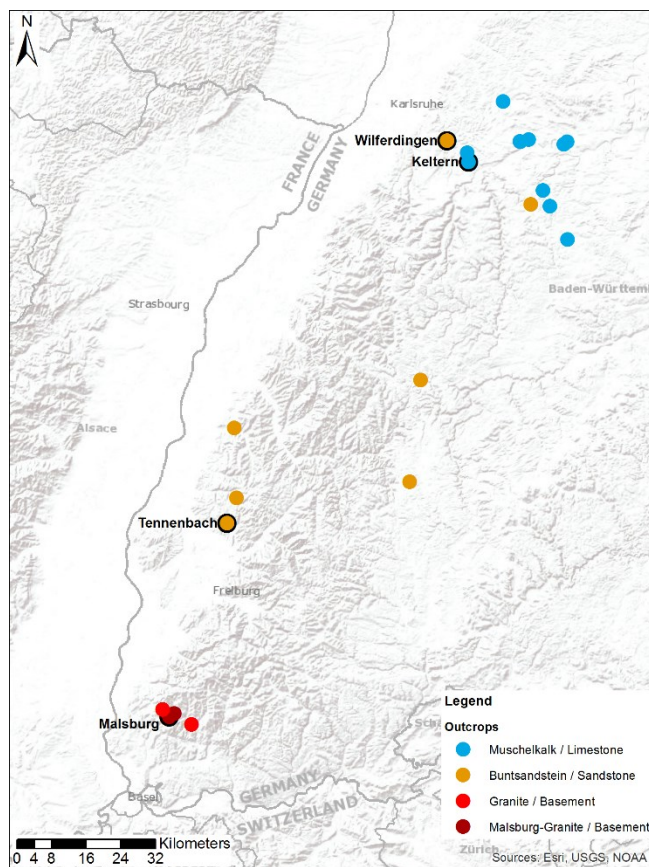


Figure 2: Map of outcrop locations in the Black Forest. Black-shadowed circles are the selected locations for sampling of the Muschelkalk (blue), Buntsandstein (yellow) and Granite (dark red).

The “Keltener Limestone” originates from an outcrop in the northern Black Forest near to Pforzheim. It is composed of shell-bearing limestone alternated with grainy parts. Density measurements shows a value of 2.67 g/m^3 which indicates low porosity and a measured hydraulic conductivity below 10^{-10} m/s . Near to the outcrop of the limestone the boundary between Muschelkalk and Buntsandstein is visible. So, the “Pfinztäler Sandstein” can be considered as part of the Upper Buntsandstein, which can be found in an outcrop near to Wilferdingen, eastern to Pforzheim. It is a fine-grained siliceous bounded sandstone with components of layered mica with a density of about 2.37 g/cm^3 . The other sandstone, the “Tennenbacher Sandstein” is part of the Middle Buntsandstein, the so called “Bausandstein”. It is characterized by a middle-grained siliceous bounded sandstone with a density of 2.17 g/cm^3 indicating a higher porosity than the “Pfinztäler Sandstein”. Measured hydraulic conductivity of about $4.9 \times 10^{-9} \text{ m/s}$ confirmed high porosity. The Crystalline Basement sample is the “Malsburg Granite” located in the southern Black Forrest and part of a batholith, originated during the variscian orogeny in the upper Lower Carboniferous. Low alteration grade and equigranular grain size distribution with generally relatively small grain sizes of the granite represent an optimal sample for our testing (Figure 3). Petrologically the “Malsburg Granite” is a biotite granite to granodiorite composed of quartz, plagioclase, kali-feldspar and biotite with a mean density is about 2.62 g/cm^3 .



Figure 3: Figure of the four rock samples that were investigated. From left to right: The “Malsburg Granite” as a bright biotite granite with a homogeneous grain size distribution. The “Keltener Limestone”, a shell-bearing limestone alternated by fine grained parts. Fine grained “Pfinztäler Sandstone” partly laminated with mica. Middle grained “Tennenbacher Sandstone”, a very homogeneous composed sandstone with high porosity.

Because of alteration and deformation processes in the deep URG, the investigations will be expanded on drilling-cores from deep wells. Further investigation will be focused on core samples of the Soultz-Sous-Forêts geothermal well EPS-1. During drilling the EPS-1 well coring started from 930 m in the Muschelkalk and ended in the Granite basement rocks in 2227 m. So, a core section of about 1297 m was provided crosscutting a part of the Muschelkalk, the hole Buntsandstein, Perm and Granite. Investigations on fractures of the Buntsandstein were carried out indicating fault zones and leading to first petrophysical parameters (Vernoux et al. 1995). Most investigations on the core samples of the Soultz borehole EPS-1 were focused on the granite, to characterize the fracture network within the crystalline basement rocks for geothermal purposes, an enhanced geothermal reservoir (EGS). Thus, studies of the fracture system (Genter 1995), alteration processes of the granite (Genter and Traineau 1992) and a lot of other studies were carried out on the granitic core of EPS-1. The core provides a continuous crosscut of the Mesozoic reservoir layers, and therefore provides the data necessary to establish a 1-D hydro mechanical model, which can be used to build up a 3-D reservoir model for hydro mechanical modeling of the entire reservoir.

3.2 Rock mechanical characterization

We first characterized the mechanical behavior of the undisturbed rocks from outcrops, and characterized the core material later on. Starting with low confining pressures and normal temperatures these parameters will be increased to reproduce reservoir conditions (p , T). First elastic parameters of the rock samples were investigated for the reservoir rocks. Fracturing studies under different loadings were performed and will be analyzed concerning the fracture style, grain size distribution, fracture roughness and width of the deformation zone. Depending on the reservoir depth, the confining pressure and temperature will increase, which influences the elastic parameters. One of our principle goals is building up a 1-D hydro mechanical model of the reservoir layers, to compare the parameters of the undisturbed host rock with the parameters observed in the faulted zones in the Muschelkalk, the Buntsandstein and the granitic basement.

3.2.1 Triaxial Testing

Mechanical characterization will be done with triaxial testing machines, which are capable to perform experiments at reservoir conditions. For depths of 5 km the confining pressure must exceed 75 MPa and temperatures should increase up to 150 °C and higher. Without any differential stress the confining pressure and axial loading will be steadily increased to the starting conditions. Afterwards the axial loading will be increased and axial displacement will be measured. These stress-strain curves can be used to describe the mechanical behavior under applied loading conditions and can be divided into several characteristic stress paths (Figure 4a). At the beginning characteristically existing fractures will be closed and pore space collapse (Paterson and Wong 2005). Subsequently, a linearly elastic section is observed, followed by a reduction of the slope caused by pre-fracturing with an inelastic / ductile behavior (Jaeger et al. 2007) and ending in rupturing at the yield strength. Depending on the rock type the stress-strain curves can differ significantly, and characterize the material as it can receive stress, which is defined as Young's modulus (E-modulus). If tests are conducted under different confining pressures Mohr-circle can be drawn with the yield strength values. This analysis establishes a criteria describing the fracturing mechanism by cohesion (C) and the slope of the covering curve as a friction coefficient (μ) (Figure 4b).

The mechanical behavior of material depends on sample characteristics and test conditions. Some are induced due to the sample (such as mineral composition, type of cementation, and porosity), and others by the testing conditions (such as confining pressure, temperature and pore pressure) (Paterson and Wong 2005). The aim of this study is to characterize the full mechanical behavior of the three stratigraphic layers by the values of the UCS, Young's modulus, cohesion (C) and the friction coefficient (μ) for different conditions.

3.2.2 Initial Results

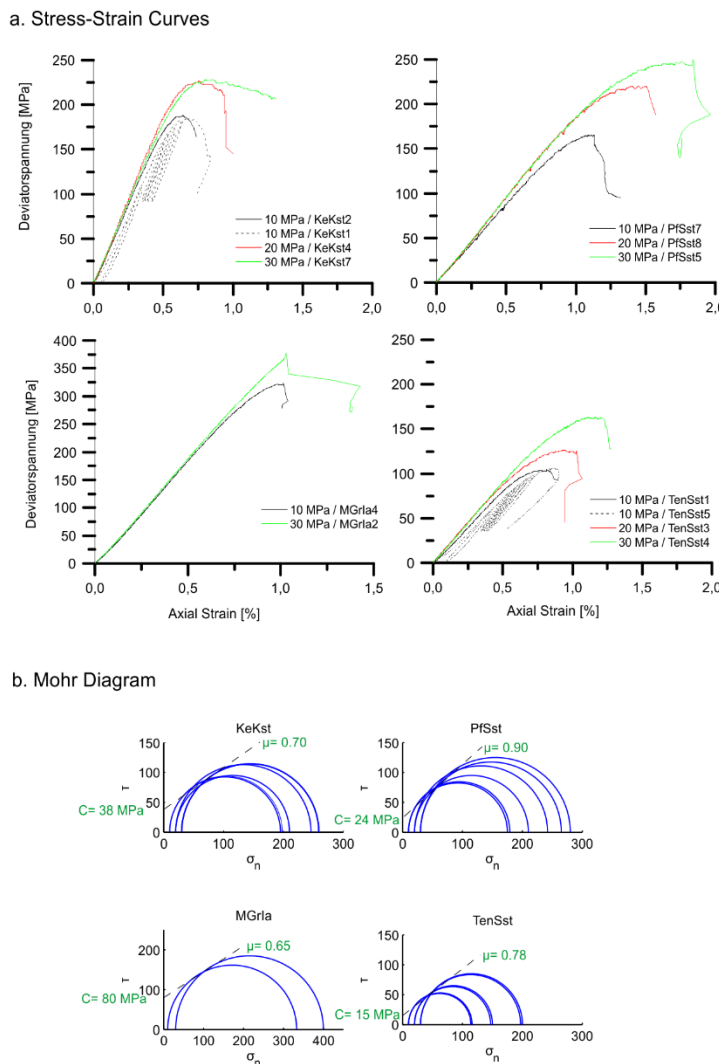
At first the experiments were started with the aforementioned samples (Section 3.1) from outcrops of the Buntsandstein, Muschelkalk and Granite with a confining pressure of 10 MPa, 20 MPa and 30 MPa. The samples had to be prepared to cylinders with a diameter of 55 mm and a length of 110 mm (Fig. 3). The first measurements define the yield strength (YS) at each confining pressure. During the second measurement, stress cycling was performed to investigate in particular the Young's modulus. Assuming the Mohr-Coulomb failure criterion, the yield strength and the confining pressure can be used to determine the cohesion (C) and the friction coefficient (μ) for every rock sample (Figure 4b).

In total, 23 triaxial tests were conducted under different confining pressures. These curves help to define phases during loading, which identify linear elastic, ductile, and brittle deformation. Rock type, especially its porosity, and the confining pressure determine the linear phase during loading. The linear elastic phase occurs over a larger range of deformation as porosity decreases. Thus, tests of the "Tennenbacher Sandstone" show a less expanded linear phase than the "Pfinztaeler Sandstone". For the Sandstones you can conclude, the lower the porosity the higher the yield strength. Additionally, a change in faulting style can be observed by different confining pressures for the limestone. At low confining pressure up to 20 MPa the rock fails abruptly, in contrast the experiments with 30 MPa confining pressure showing an extended phase with brittle deformation. Both rocks, the "Keltener Limestone" and the "Malsburg Granite," show a vast area with linearly elastic behavior, which is characteristic for low porosity rocks. Depending on the rock type, the Young's modulus can vary significantly. Both sandstones show a Young's modulus of about 20 to 25 GPa, the limestone of about 37 to 42 GPa and the granite of about 37 to 40 GPa. Triaxial tests under various confining pressures show a dependency of the Young's modulus on the test conditions (Table 1). Mohr-Coulomb circles indicate that the sandstones possess almost the same coefficient of internal friction, but differ particularly in their Cohesion. Comparing the limestone and the granite the same phenomena can be observed. Granites have a much higher cohesion but do not differ in the friction coefficient.

So far, the first samples of the outcrops in the Black Forest were analyzed under relatively low confining pressure (10 -30 MPa) and under normal temperatures. These samples show different results of rock strength and Young's modulus under varying test conditions. Further analyses will be conducted with increased confining pressure and temperature up to 100 MPa and 160 °C, to simulate reservoir conditions in order to get better in-situ mechanical parameters.

Table 1: Composition of the first triaxial tests of the analyzed rock samples from outcrops in the Black Forest. Mechanical parameters of Cohesion, Coefficient of internal friction / Friction angle and Young's Modulus were analyzed.

	Keltener Limestone (KeKst)	Pfinztaeler Sandstone (PfSst)	Tennenbacher Sandstone (TenSst)	Malsburger Granite (MGrIa)
Cohesion [MPa]	38	24	15	80
Coefficient of internal friction / Friction angle	0.70 / 35°	0.90 / 42°	0.78 / 38°	0.65 / 33°
Young's Modulus [GPa]	42 (10 MPa) 37 (20 MPa)	20 (10 MPa) 24 (20 MPa) 25 (30 MPa)	20 (10 MPa) 21 (20 MPa) 21 (30 MPa)	37 - 40 (10 MPa)

**Figure 4: a.) Stress- Strain Curves of the four rock types with 10 MPa, 20 MPa and 30 MPa confining pressure. b.) Mohr- Coulomb Diagrams of the triaxial tests with the cohesion and friction coefficient of the coulomb failure criterion.**

3.3 Future Investigation

Simultaneously, samples from the EPS-1 well in Soultz-sous-Forêts will be analyzed to study the hydro-mechanical parameters near and within fault zones. V_p and V_s velocities can provide the dynamic Young's modulus. The density, porosity and micro fracture analyses can help to describe the deformation grade. Analyses of triaxial tests can give us strength data, the static Young's modulus and help to classify the mechanical parameters. The aim of this study is to roughly characterize the typical reservoir rocks in the URG and to develop a 1-D hydro mechanical model. On the basis of this model a 3D- geomechanical model with included fault structures will be developed for the geothermal reservoir in the URG. This model will show the stress distribution in the

reservoir under assumed parameters. It can further help to localize “sweet spots” under mechanical issues or improve borehole stability, respectively help to determine the target point of the borehole.

4. CONCLUSION AND GEOMECHANICAL MODELING

Mechanical triaxial tests of undeformed rock samples from outcrops in the Black Forest give us the first insight into the typical mechanical behavior of different rock types. We see porosity and pre-fracturing as the most significant parameters as well as mineralogy, grain size distribution and diagenetic processes. Under rising confining pressure, yield strength and Young’s modulus increase. Further analyses will be performed under reservoir conditions with a confining pressure of 100 MPa and temperatures of 160°. One of our central aims is to establish a 1-D hydro-mechanical model of the geothermal reservoir sections in the URG. This will be analyzed on the core of the well EPS-1 of the Soultz-sous-Forêts geothermal project, which consists of altered faulted rocks, diagenetic marked faulted rocks as well as undeformed host rocks. Additionally, investigations on natural fault zones in underground mines are planned, which give us insights into fault structures and their hydro-mechanical parameters. This wide range of different rock types of faulted to undeformed rocks in different scales enables us to transfer the parameters to a 3-D geomechanical reservoir model in the URG.

ACKNOWLEDGEMENT

The research project is integrated in the project StörTief, supported by the German Federal Ministry for Economic Affairs and Energy (BMWi, no: 0325623C).

REFERENCES

Brudy M, Zoback MD (1993) Compressive and Tensile Failure of Boreholes Arbitrarily-Inclined to Principal Stress Axes - Application to the KTB Boreholes, Germany. *International Journal of Rock Mechanics and Mining* 30 (7):1035-1038. doi:10.1016/0148-9062(93)90068-O

Bucher K, Stober I (2010) Fluids in the Upper Continental Crust. In: *Frontiers in Geofluids*. Wiley-Blackwell, pp 241-253. doi:10.1002/9781444394900.ch17

Byerlee J (1978) Friction of Rocks. *Pure and Applied Geophysics* 116 (4-5):615-626. doi:10.1007/Bf00876528

Caine JS, Bruhn RL, Forster CB (2010) Internal structure, fault rocks, and inferences regarding deformation, fluid flow, and mineralization in the seismogenic Stillwater normal fault, Dixie Valley, Nevada. *Journal of Structural Geology* 32 (11):1576-1589. doi:DOI 10.1016/j.jsg.2010.03.004

Chinnery MA (1965) Secondary Faulting: 1. Theoretical Aspects. *Canadian Journal of Earth Sciences* 3:163-174

Faulkner DR, Jackson CAL, Lunn RJ, Schlische RW, Shipton ZK, Wibberley CAJ, Withjack MO (2010) A review of recent developments concerning the structure, mechanics and fluid flow properties of fault zones. *Journal of Structural Geology* 32 (11):1557-1575. doi:DOI 10.1016/j.jsg.2010.06.009

Faulkner DR, Lewis AC, Rutter EH (2003) On the internal structure and mechanics of large strike-slip fault zones: field observations of the Carboneras fault in southeastern Spain. *Tectonophysics* 367 (3-4):235-251. doi:DOI 10.1016/S0040-1951(03)00134-3

Genter A, Trainau H (1992) Hydrothermally Altered and Fractured Granite as an HDR Reservoir in the EPS-1 Borehole, Alsace, France. Paper presented at the Proceedings, Seventeenth Workshop on Geothermal Reservoir Engineering Stanford University, Stanford, California, January 29-31, 1992

Genter AT, H. (1995) Fracture analysis in granite in the HDR geothermal EPS-1 well, Soultz-Sous-Forêts, France. BRGM,

Gudmundsson A, Simmenes TH, Larsen B, Philipp SL (2010) Effects of internal structure and local stresses on fracture propagation, deflection, and arrest in fault zones. *Journal of Structural Geology* 32 (11):1643-1655. doi:10.1016/j.jsg.2009.08.013

Homberg C, Hu JC, Angelier J, Bergerat F, Lacombe O (1997) Characterization of stress perturbations near major fault zones: Insights from 2-D distinct-element numerical modelling and field studies (Jura mountains). *Journal of Structural Geology* 19 (5):703-718. doi:10.1016/S0191-8141(96)00104-6

Jaeger J, Cook NG, Zimmerman R (2007) *Fundamentals of Rock Mechanics*. Wiley-Blackwell,

Mazurek M (1998) Geology of the crystalline basement of Northern Switzerland and derivation of geological input data for safety assessment models. Kümmerly & Frey, Bern

Mazurek M, Jakob A, Bossart P (2003) Solute transport in crystalline rocks at Aspo: I: Geological basis and model calibration. *Journal of Contaminant Hydrology* 61 (1-4):157-174

Paterson M, Wong T-f (2005) *Experiments in Rock Deformation - The Brittle Field*. Springer, Heidelberg

Peska P, Zoback MD (1995) Compressive and Tensile Failure of Inclined Well Bores and Determination of in-Situ Stress and Rock Strength. *Journal of Geophysical Research - Solid Earth* 100 (B7):12791-12811. doi:10.1029/95jb00319

Reinecker J, Tingay M, Muller B, Heidbach O (2010) Present-day stress orientation in the Molasse Basin. *Tectonophysics* 482 (1-4):129-138. doi:10.1016/j.tecto.2009.07.021

STMWIVT BSfW, Infrastruktur, Verkehr und Technologie (2010) *Bayerischer Geothermieatlas - Hydrothermale Ernergiegewinnung*. München

Stober I (2013) Geothermal fluid and reservoir properties in the Upper Rhine Graben, Europe. Paper presented at the Sustainable Earth Sciences 2013, Pau, France,

Stober I, Fritzer T, Obst K, Schulz R (2011) Tiefe Geothermie - Nutzungsmöglichkeiten in Deutschland. vol 3. Aufl. Bundesministerium für Umwelt, Naturschutz und Reaktorsicherheit, Berlin

Su S, Stephansson O (1999) Effect of a fault on in situ stresses studied by the distinct element method. International Journal of Rock Mechanics and Mining Sciences 36 (8):1051-1056. doi:10.1016/S1365-1609(99)00119-7

Vernoux JF, Genter A, Razin P, Vinchon C (1995) Geological and petrophysical parameters of a deep fractured sandstone formation as applied to geothermal exploitation, EPS-1 borehole, Soultz-sous-Forêts.

Yale DP (2003) Fault and Stress magnitude controls on variations in the orientation of in situ stress. In: Ameen M (ed) Fracture and In-Situ Stress Characterization of Hydrocarbon Reservoirs, vol Special Publications. Geological Society, London, pp 55 - 64.